Food Research International 119 (2019) 725–732

Contents lists available at ScienceDirect

Food Research International

journal homepage: www.elsevier.com/locate/foodres

Spatial distributions of furan and 5-hydroxymethylfurfural in unroasted and roasted *Coffea arabica* beans

Kristen L. Fowble[a], Koji Okuda[b], Robert B. Cody[b], Rabi A. Musah[a,*]

[a] University at Albany—State University of New York, Department of Chemistry, 1400 Washington Avenue, Albany, NY 12222, USA
[b] JEOL, Inc., 11 Dearborn Road, Peabody, MA 01960, USA

ARTICLE INFO

Keywords:
Coffea arabica beans
Furan
5-Hydroxymethylfurfural
Small-molecule spatial distributions
Laser ablation direct analysis in real time imaging-mass spectrometry (LADI-MS)
Imaging mass spectrometry

ABSTRACT

For the first time, the spatial distributions of the highly volatile compounds furan and 5-hydroxymethylfurfural (HMF) have been determined in cross sections of green and roasted *Coffea arabica* beans. The image maps were revealed by laser ablation DART imaging mass spectrometry (LADI-MS). The presence of these compounds was independently confirmed by GC–MS as well as argon DART-MS. Quantification of furan by GC–MS was completed with the final concentrations in roasted and unroasted beans determined to be 96.5 and 4.1 ng/g, respectively. Furan was observed to be distributed throughout the tissue of both green and roasted beans, while HMF was localized to the silver skin in green beans. Following roasting, the appearance of HMF was more diffuse. The implications of the broad distribution of furan on the one hand, and localization of HMF on the other, are discussed.

1. Introduction

Freshly brewed coffee elicits in humans a composite of sensory experiences that engage the faculties of sight (color and consistency), smell (from the fragrance attributes of emitted volatiles) and taste, evoking such descriptors as rich, bold, dark, full-bodied, warm, robust, and the like. Aside from the influence of the chemicals whose appearance is defined by the genetic makeup of the specific coffee species, as well as the cultivar and growth conditions, the organoleptic properties of roasted coffee arise from compounds formed through a cascade of heat-promoted chemical transformations including Maillard and Strecker degradation reactions, and caramelization that occur more or less simultaneously during heat processing. The precursors for the formation of these compounds include sugars, amino acids, vitamins, lipids and fatty acids. The identities of the compounds produced and their formation levels are impacted by the relative concentrations of the precursors themselves. However, it is likely that they are also influenced by the relative distributions of the precursors within the bean, although this latter possibility has been little investigated because information on their tissue localization remains largely unknown. Several reports have appeared detailing both the health benefits and detriments of coffee brews and their constituent components (Arisseto, Vicente, Ueno, Tfouni, & Toledo, 2011; Monien, Engst, Barknowitz, Seidel, & Glatt, 2012; Zanin, Corso, Kitzberger, Scholz, & Benassi, 2016). While some compounds have been documented to impart health benefits, such as chlorogenic acids which exhibit antioxidant and anti-inflammatory effects (Zanin et al., 2016), others are perceived to have negative health impacts (IARC, 1995; Monien et al., 2012; Neuwirth et al., 2012; Peterson, 2013).

Although both are purported to contribute to the sensory properties of the foods in which they appear (Maga & Katz, 1979), furan and 5-hydroxymethylfurfural (HMF) are two compounds whose detection in coffee has raised concerns. Their concentrations in roasted coffee have been observed to range from 38.7–51.341 ng/g and 0.452–6.27 mg/g respectively (Becalski, Halldorson, Hayward, & Roscoe, 2016; Moon & Shibamoto, 2009; Quarta & Anese, 2012; Sijia, Enting, & Yuan, 2014). Both compounds can be derived from several reactions involving a range of different precursors and/or intermediates (Capuano & Fogliano, 2011; Crews & Castle, 2007). HMF has been shown to induce mutagenic and genotoxic effects in bacteria and human cells and promote colon and liver cancer in rats and mice (Monien et al., 2012), although it remains unclear if these effects extend to humans (Capuano & Fogliano, 2011). HMF formation in foods has been found to be affected by sugar type, pH, water content and the presence of divalent cations (Gökmen, Açar, Köksel, & Acar, 2007; Gökmen & Şenyuva, 2007; Kroh, 1994). HMF can be formed from the caramelization of sugars such as sucrose (Kroh, 1994) or fructose (Roman-Leshkov, Chheda, & Dumesic, 2006) through formation of a fructofuranosyl cation under thermal treatment and acidic catalysis. Glucose and fructose can also generate HMF through the formation of a dicarbonyl

* Corresponding author.
E-mail address: rmusah@albany.edu (R.A. Musah).

https://doi.org/10.1016/j.foodres.2018.10.052
Received 20 July 2018; Received in revised form 15 October 2018; Accepted 18 October 2018
Available online 19 October 2018
0963-9969/

intermediate, 3-deoxyglucosone (3-DG), from the Maillard reaction and caramelization (Kato, Hayase, Shin, Oimomi, & Baba, 1989).

Several mechanisms for the formation of furan have been discovered, largely through studies of various model systems (Crews & Castle, 2007; Limacher, Kerler, Conde-Petit, & Blank, 2007; Limacher, Kerler, Davidek, Schmalzried, & Blank, 2008; Maga & Katz, 1979; Perez Locas & Yaylayan, 2004), food-simulating systems (Owczarek-Fendor et al., 2010; Owczarek-Fendor et al., 2011) and foods themselves (Limacher et al., 2007). Furan is classified as a known carcinogen in rats (Neuwirth et al., 2012), and a possible carcinogen in humans (Group 2B) (IARC, 1995). Its harmful effects have been proposed to be a consequence of cytochrome P450-mediated oxidation which furnishes a reactive *cis*-butene-1,4-dial metabolite which in turn can bind to various cellular components (Peterson, 2013).

Concerns over the potential harmful effects of furan and HMF in foods and beverages have spurred efforts to develop methods to reduce their concentrations or eliminate them altogether (Anese, Bot, & Suman, 2014; Quarta & Anese, 2012). However, this remains a formidable challenge because both can be formed from several precursors. In principle, one approach to the systematic development of mitigating strategies to reduce or eliminate the formation of compounds of concern is to better understand the areas within the bean where the molecules and their precursors reside, as the localization of these compounds might suggest approaches for their removal. However, little is known about the spatial distributions of the molecular components in green and roasted coffee beans. Previous investigations of the tissue specific appearance of small molecules within *Coffea* spp. have focused on bulk materials including beans, bark, leaves, and roots of *C. arabica* plants (Somorin, 1974; Zheng & Ashihara, 2004), thus losing spatial distribution information. A number of more recent studies have sought to address this through alternative methods. For example, tissular distribution of pentacyclic diterpenoids in coffee beans was accomplished by Dias et al. through manual separation of the different tissues followed by analysis of each (Dias et al., 2010). Conéjéro et al. were able to determine the tissue localization of chlorogenic acid and mangiferin in leaf cross-sections of several members of the *Coffea* genus by exploiting their autofluorescence characteristics (Conejero, Noirot, Talamond, & Verdeil, 2014). The information gleaned from these efforts implies that imaging mass spectrometry could serve as a powerful tool for determination of the tissular localization of a broad variety of small molecules within the complex coffee bean matrix.

In this study, we applied the imaging mass spectrometry technique of laser ablation direct analysis in real time imaging-mass spectrometry (LADI-MS) to the detection of small molecules in unroasted and roasted *Coffea arabica* beans. This approach has a number of advantages that lend themselves well to the detection of small molecules in complex matrices (Fowble et al., 2017) such as coffee beans. Among other things, the experiment does not require a vacuum (all experiments are conducted in open air), solvent, sample fixation or embedment, or a matrix. Furthermore, the technique accommodates irregularly-shaped samples (i.e. there is no need for the sample to be analyzed in thin slices), and no sample pre-treatment steps are required. Herein, we describe the use of LADI-MS for the detection of the highly volatile compounds furan and HMF in unroasted and roasted *C. arabica* beans to reveal for the first time the spatial distributions of each, and determine the impact of roasting on their distributions within the tissue.

2. Materials and methods

2.1. Chemicals

Furan standard and chlorobenzene were purchased from Sigma-Aldrich (St. Louis, MO, USA). 5-Hydroxymethylfurfural was purchased from Fisher Scientific (Hampton, NH, USA). High-purity helium and argon gases were obtained either from Airgas (Albany, NY, USA) or Matheson (Manchester, NH, USA).

2.2. Coffee beans

Unroasted (green) and roasted *Coffea arabica* beans from Antigua, Colombia were purchased from Uncommon Grounds (Albany, NY, USA). The green unroasted beans were roasted onsite at Uncommon Grounds using a Probat solid drum coffee roaster. Unroasted beans were introduced into the drum when it reached a temperature of 210 °C. The drum temperature was then raised 0.35 °C min^{-1} for 11 min to a final temperature of 213.89 °C after which they were removed from the drum and stirred until they reached room temperature. The roasting parameters were those used at the Uncommon Grounds facility using the in-house coffee roaster, and are identical to those used for coffee beans sold to customers.

2.3. Argon direct analysis in real time-high-resolution mass spectrometry (DART-HRMS) analysis

Argon DART-HRMS experiments were conducted using a JEOL AccuTOF-LP 4G mass spectrometer (JEOL USA, Inc., Peabody, MA) with a resolving power of 10,000 FWHM, coupled to a DART-SVP ion source (Ionsense LLC, Saugus, MA). Chlorobenzene was used as a dopant for analyses and was infused by a syringe pump at a flow rate of 9 μL min^{-1} through deactivated fused-silica tubing positioned at the open-air gap. The DART ion source was operated in positive ion mode with a gas heater temperature of 400 °C and a gas flow rate of 2 L min^{-1}. The mass spectrometer was operated with an orifice 1 voltage of 20 V and orifice 2 and ring lens voltages of 5 V each. The ion guide voltage was set to 500 V to allow for the detection of ions above *m/z* 50. A roasted coffee bean was crushed to produce a number of smaller pieces for analysis. Tweezers were used to suspend portions of the roasted coffee bean in the open-air sample gap between the DART ion source and the AccuTOF mass spectrometer inlet. Multiple pieces of two coffee beans were analyzed and the spectra were averaged together.

2.4. Coffee bean extract sample preparation

2.4.1. Extract for furan confirmation

Unroasted and roasted coffee beans were crushed. One gram of crushed unroasted coffee beans was suspended in 10 mL of room temperature water in a capped 22 mL vial with a septum-containing screw cap (Supelco, Bellefonte, PA, USA) and placed in a hot water bath (95 °C) for 10 min. The vial was removed, shaken for 30 s to establish gas/liquid equilibration, and allowed to cool for 10 min before headspace extraction. A Pressure-Lok® precision analytical syringe (Supelco, Bellefonte, PA, USA) was used to withdraw 500 μL of the coffee extract headspace for injection. The vial was reheated in the same manner two more times for triplicate analysis. The vials were kept capped for the entire procedure to prevent furan from evaporating. This process was repeated using roasted coffee beans.

2.4.2. Extract for HMF confirmation

Unroasted and roasted coffee beans were ground and 10 mg of each were placed in separate 2 mL amber glass GC vials (Agilent, Santa Clara, CA, USA). A methanol:dichloromethane 1:1 solution (1 mL) was added to each vial. The extracts were allowed to stand at room temperature overnight before analysis. A small aliquot (200 μL) was taken from the extract to be used for GC–MS analysis.

2.5. Preparation of standard solutions

A calibration series for furan was prepared by creating 10 ng/g, 50 ng/g, and 100 ng/g standard solutions of furan in 10 mL of water in 22 mL septum-containing capped vials. Furan standard was refrigerated before opening and once the vials were capped, the caps were not removed during analysis in order to prevent evaporation of furan. A

20 μg/g standard solution of HMF in 200 μL of 1:1 methanol:dichloromethane was prepared.

2.6. GC–MS analysis

GC–MS analyses were conducted using a JMS-T200GC AccuTOF GCx (JEOL USA, Inc., Peabody, MA) mass spectrometer equipped with a 7890B Agilent GC. GC–MS data processing was performed using msAxel software (JEOL USA, Inc., Peabody, MA).

2.6.1. Furan confirmation

The headspace (500 μL) was analyzed using an HP-FFAP column (30 m × 0.25 mm, 0.25 μm) (Agilent, Santa Clara, CA, USA) under the following conditions: oven temp: 30 °C, held for 10 min, raised linearly at a rate of 30 °C min^{-1} to 240 °C and held there for 9 min; inlet temperature: 200 °C; carrier gas: helium, with a flow rate of 1 mL min^{-1}; inlet mode: split 15:1; ionization mode: EI+, 70 V, 300 μA. Furan standards (including a blank) were analyzed once and coffee samples were run in triplicate.

2.6.2. HMF confirmation

Of the 200 μL solution, only 1 μL was injected into the GC. The sample was analyzed using a HP-FFAP column (30 m × 0.25 mm, 0.25 μm) under the following conditions: oven temp: 40 °C, held for 1 min, raised linearly at a rate of 15 °C min^{-1} to 240 °C and held there for 10 min; inlet temperature: 230 °C; carrier gas: helium, with a flow rate of 1 mL min^{-1}; inlet mode: split 50:1; ionization mode: EI+, 70 V, 300 μA. The HMF standard was analyzed once, and coffee extracts were analyzed in triplicate.

2.7. Sample preparation of coffee beans for LADI-MS analysis

Unroasted and roasted coffee beans were sliced in half, transverse wise, using a razor blade. The bean halves were placed (separately) onto a bed of Loctite Fun Tak® mounting putty with the cut face exposed. The putty was then placed on the sample plate which was then inserted into the laser ablation system air-tight sample chamber for analysis.

2.8. Light microscopy imaging of unroasted coffee beans

A Nikon stereozoom SMZ800 microscope coupled to a Nikon DS Fi2 microscope camera was used to collect light microscopy images of the transverse cross-section of an unroasted coffee bean.

2.9. LADI-MS analysis

LADI-MS was set up as previously described (Fowble et al., 2017). Briefly, ion images were acquired using an ESL NWR213 laser ablation imaging system (ESL, Bozeman, MT, USA) coupled with a direct analysis in real time (DART) ion source (IonSense, Saugus, MA) and JEOL AccuTOF high-resolution mass spectrometer (HRMS) (JEOL USA, Peabody, MA). The mass spectrometer was operated with an orifice 1 voltage of 20 V and orifice 2 and ring lens voltages of 5 V in positive ion mode with a scan collection rate of 0.6 s $scan^{-1}$. The resolving power of the HRMS used was 6000 FWHM. The rate of the DART ion source helium flow was 2.0 L min^{-1} with a heater temperature of 350 °C. An ion guide voltage of 600 V was used for the detection of ions above *m/z* 60. Polyethylene glycol (PEG) was used as a reference standard for the calibration of the collected spectra. TSSPro3 software (Shrader Software Solutions, Grosse Pointe Park, MI, USA) was used for peak calibration and peak centroiding. Reconstructed ion chromatograms were created for each of the ions of interest and imported into Iolite imaging software (University of Melbourne, AUS). Mass spectral analysis, elemental composition determination and isotope analysis were performed using Mass Mountaineer software (Massmountaineer.com, Portsmouth, NH, USA).

The following laser parameters were used: laser beam energy density (fluence) = 21 J cm^{-2}; laser frequency = 20 Hz; scan speed = 65 μm s^{-1}; spot size = 70 × 70 $μm^2$; line width = 60 μm; and He flow rate = 600 mL min^{-1}. Based on the experimental parameters used, the spatial resolution attained was 154.5 × 70 $μm^2$ (i.e. [*x*-spot size + (cell washout time (0.7 s) * scan speed) + (MS scan rate (0.6 s $scan^{-1}$) * scan speed)] x *y*-spot size).

3. Results and discussion

3.1. Detection of furan and HMF in roasted coffee beans by dopant-assisted argon direct analysis in real time-high-resolution mass spectrometry (DART-HRMS)

A prerequisite for determination of the spatial distributions of molecules by LADI-MS is the ability to observe them in the sample of interest by DART-HRMS. Conventional DART-HRMS relies on metastable helium which when exposed to atmospheric water results in the formation of protonated water clusters via Penning ionization. Proton transfer from the clusters to the analytes serves as the ionization mechanism for species detected in positive ion mode. This process of analyte ionization has two consequences. The first is that only species whose proton affinities are greater than that of water are ionized. Therefore, it is possible that molecules may be present but not detected because their proton affinities are too low. The second is that although a range of molecules may be detected because their proton affinities are greater than that of water, the relative intensities of their representative peaks might not necessarily reflect their relative amounts. This is because peak intensity is also correlated to proton affinity. For example, for two molecules that are present in the same amount, but which have different proton affinities, that with the higher proton affinity is more efficiently ionized and therefore its peak exhibits a greater intensity. For these reasons, amines, which generally have relatively high proton affinities, dominate DART-HRMS spectra when they are present. In the case of coffee, the presence of caffeine and other alkaloids has the potential to dominate the mass spectrum and make the presence of other compounds of interest less apparent. We circumvented this issue by utilizing argon DART-HRMS with chlorobenzene as a dopant. In contrast to helium DART-HRMS, this approach generates ions by Penning ionization, followed by proton and/or charge transfer from the dopant, with charge transfer being the favored mechanism. Thus, high proton affinity analytes such as caffeine do not dominate the argon DART mass spectrum and other compounds (with lower ionization energies than chlorobenzene) such as furan and HMF, can be readily detected. Furan and HMF are ionized by an initial charge transfer from the dopant chlorobenzene followed by proton transfer from other ions in the mixture in the open-air gap between the ion source and the mass spectrometer inlet. A typical argon DART-high-resolution mass spectrum collected over the range *m/z* 50–250 is presented in Fig. 1. The inset shows an expansion of the *m/z* 60–75 region which features the high-resolution mass of protonated furan at *m/z* 69.0306, and the peak at *m/z* 127.0424 is representative of protonated HMF. The other high intensity peaks at nominal *m/z* 94, 108, 112 and 194 are representative of phenol, anisole, chlorobenzene and caffeine, respectively. The phenol and anisole are derived from the tubing used to introduce the dopant. The identities of both furan and HMF were independently confirmed by GC–MS and comparison of their fragmentation patterns to those of authentic standards. The detection of furan and HMF by DART-HRMS indicated that in principle, their spatial distributions could be mapped by LADI-MS.

3.2. Independent confirmation of furan in unroasted and roasted coffee beans by GC–MS

Although many studies have reported that furan is a product of

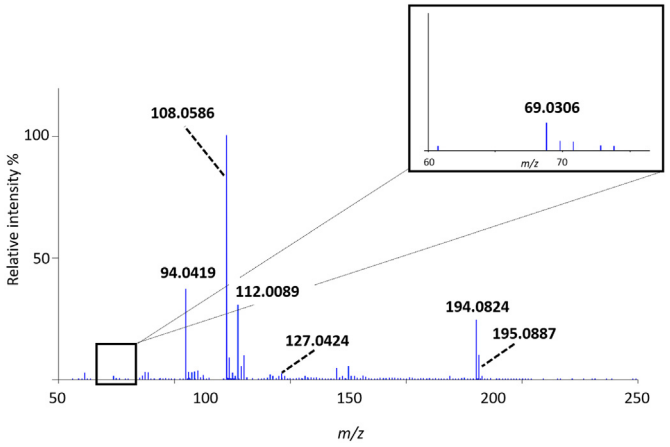

Fig. 1. A representative dopant-assisted argon DART-HRMS mass spectrum of a roasted coffee bean over a mass range of *m/z* 50–250. The inset (upper right corner) is an expansion of the mass spectrum in the range of nominal *m/z* 60–75. The peaks at *m/z* 69.0306 and 127.0424 are consistent with those of the protonated masses of furan and 5-hydroxymethylfurfural, respectively.

roasting and is found readily in roasted beans (Arisseto et al., 2011; Maeztu et al., 2001), only one has reported detection of furan in green unroasted coffee beans, albeit at very low levels (Kuballa, Stier, & Strichow, 2005). We were able to independently confirm the results of previous studies that showed the presence of furan in both unroasted and roasted coffee beans.

A gas-tight syringe was used to sample the headspace of coffee bean extracts for its subsequent analysis using GC-TOF-MS. Furan was detected with a retention time of 2.27 min in each standard solution. The areas under the peaks were integrated for each standard solution and a calibration curve was created for the quantification of furan in coffee beans. The standard curve, ranging in concentrations from 0 ng/g to 100 ng/g of furan is shown in Fig. 2. The limit of detection and limit of quantification were determined to be 0.94 ng/g and 3.12 ng/g, respectively. Furan was detected in the headspace of the solutions of both the unroasted and roasted coffee bean extracts, also at 2.27 min. The resulting GC chromatograms (of one of the replicates) are illustrated in

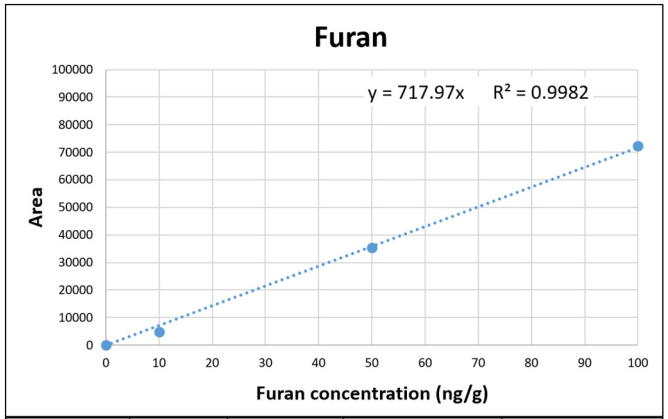

Sample	Average Area	Standard Deviation	Coefficient of Variation (%)	Calculated Concentration
Unroasted	2934.7	71.5	2.4	4.1 ng/g
Roasted	69292.4	3110.1	4.5	96.5 ng/g

Fig. 2. The standard curve for the quantification of furan (peak area v. concentration (ng/g)) over a range of 0–100 ng/g. The R^2 value for the curve is 0.9982. The average peak areas, standard deviations, coefficients of variation and calculated concentrations of furan for the unroasted and roasted coffee beans are shown.

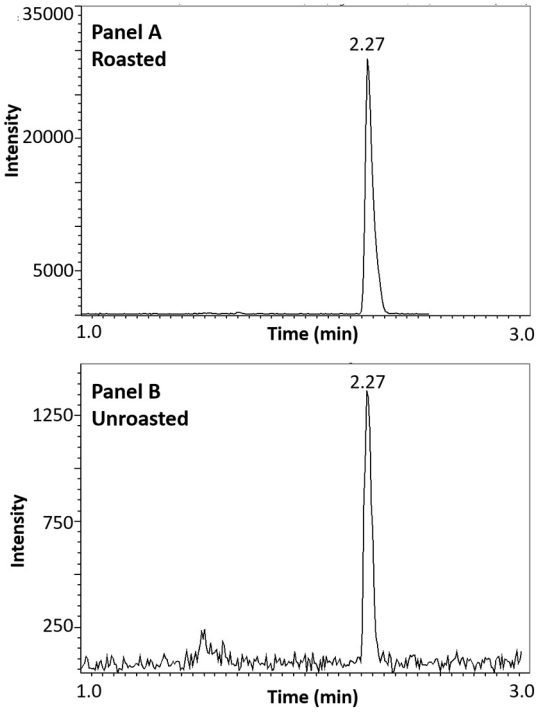

Fig. 3. The GC extracted ion chromatograms (EIC) for furan in the roasted and unroasted coffee bean headspace gases in the time range of 1–3 min are shown in Panels A and B, respectively.

Fig. 3 Panels A and B, showing an expansion of the extracted ion chromatogram for furan in the 1–3 min range. The roasted and unroasted GC traces appear in Panel A and Panel B, respectively. Analysis of the area under the curve compared to the standard curve (Fig. 2) furnished furan concentrations in both the unroasted and roasted coffee beans of 4.1 ng/g and 96.5 ng/g, respectively. The coffee bean samples were run in triplicate, with coefficients of variation of less than 5% in both unroasted and roasted beans (Fig. 2). While it could be argued that furan detected in unroasted beans could be formed during the heating of the coffee bean extract prior to headspace sampling, the consistency between the three analyses that required reheating of the same coffee bean extract suggests that little to no furan was created through the heating of the samples. The results are consistent with the report that observed the presence of low quantities of furan in unroasted beans (Kuballa et al., 2005). The detection of furan in the green beans, however, does not negate the finding that roasting is a major contributor to its formation. As confirmed here, the level of furan was found to be significantly higher in the beans which had undergone the roasting process.

3.3. Independent confirmation of HMF in unroasted and roasted coffee beans by GC–MS

There are several reports of the detection of HMF in roasted coffee samples (Anese, 2015; Lee et al., 2017; Lee, Cheong, Curran, Yu, & Liu, 2016). Many focus on how the roasting process and steps taken by the consumer affect HMF levels in brewed coffee. A few groups have shown that the concentration of HMF decreases the longer the beans are roasted (Anese, 2015; Lee et al., 2016). This could be due to the compound's instability and its role as a precursor for other molecules. Although many studies have determined the presence of HMF in roasted beans and brews, there are conflicting results on its presence in green unroasted beans, with only one confirming its detection (Lee et al., 2017).

A direct injection of 1 μL of the methanol:dichloromethane 1:1 extract was used for the GC–MS analysis. HMF was detected at 14.78 min

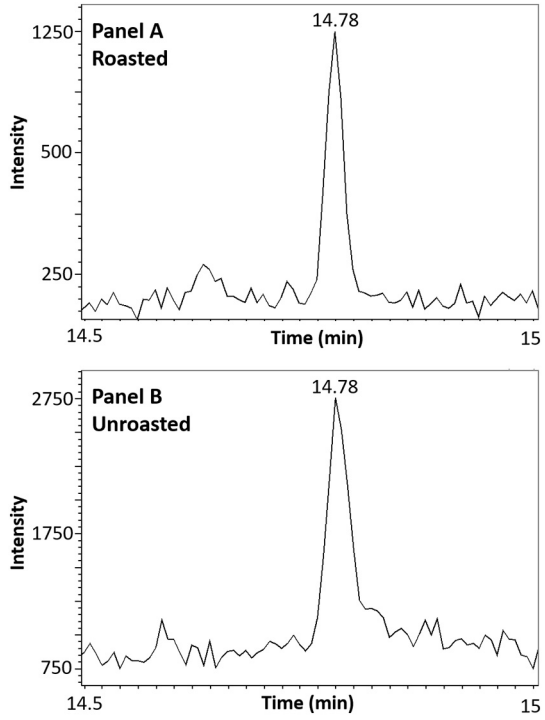

Fig. 4. The GC extracted ion chromatograms (EIC) for HMF in the roasted and unroasted coffee bean 1:1 methanol:dichloromethane extracts in the time range of 14.5–15 min. These appear in Panels A and B, respectively.

in the standard solution, the unroasted coffee extract and the roasted coffee extract. The extracted GC chromatograms of HMF in roasted and unroasted coffee bean extracts are shown in Fig. 4 Panels A and B, respectively in the time range of 14.5–15 min, within which HMF elutes. Although there are conflicting results in the literature on the presence of HMF in unroasted beans, our results confirm its presence in both the roasted and unroasted bean extract.

3.4. Ion images acquired by LADI-MS

To facilitate the interpretation of the areas within the coffee bean where the compounds of interest were localized, Fig. 5 shows a light microscopy image of an unroasted coffee bean to illustrate its internal anatomy. The apparent loop within the transverse cross-section is referred to as the perisperm or silver skin (A), while the surrounding tissue comprises the endosperm (B) (De Castro & Marraccini, 2006). The perisperm which disintegrates during the roasting process, also covers the exterior of the unroasted coffee beans (A). These terms will be used to describe the locales of the compounds of interest that were determined by LADI-MS.

Fig. 6 shows the color-overlaid ion images that illustrate the observed spatial distributions of furan and HMF in the transverse cross-sections of unroasted (top row) and roasted (bottom row) coffee beans. The dashed line around each image represents the periphery of the beans. At the right of each image is a color scale bar ranging from black to yellow, representative of a low or zero intensity to a high intensity of the indicated ion, respectively. As detection of molecules by helium DART-HRMS is dependent on a molecule's proton affinity and not the relative amount of the observed analyte that is in a sample, the scale bars of the various ion images cannot be used to estimate the relative concentrations of the analytes in the coffee beans in comparison with another, and are only indicative of the varying relative concentration of that particular ion across the bean's tissue. The top two Panels A and B are ion images representative of furan and HMF respectively in an unroasted coffee bean. The bottom row of images (Panels C and D) is of

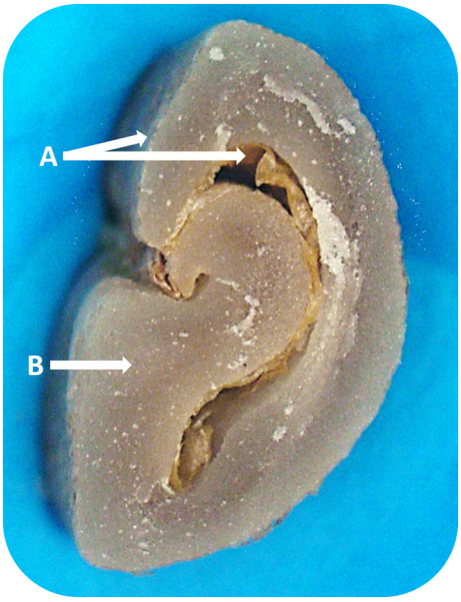

Fig. 5. A light microscopy image of a transverse cross-section of a green (unroasted) coffee bean. The perisperm (silver skin) is the loop within the center of the coffee bean and a thin layer covering the outside (A). The surrounding tissue comprises the endosperm (B).

the same compounds in a roasted coffee bean. The furan ion images show that this molecule is distributed throughout the endosperm in both the unroasted and roasted coffee beans, with higher levels located in some areas of the silver skin and relatively lower levels at the top of the unroasted bean ion image. However, it should be noted that these ion images are not normalized to the same scale because of the large difference between the levels of furan in the unroasted versus roasted bean. This difference in furan levels is reflected in the GC–MS data showing that the concentration of furan in the roasted and unroasted beans is 96.5 ng/g and 4.1 ng/g, respectively. After the LADI-MS analyses, there was a yellow discoloration observed on the surface of the unroasted bean. This could be interpreted as “roasting” caused by the laser ablation system. However, with the confirmation of furan in both unroasted and roasted beans by GC–MS, and with the consistency between the results for all three injections (Fig. 2), the effect of the laser in generating furan is deemed to be negligible. Panels B and D illustrate the non-homogenous spatial distributions of HMF in the unroasted and roasted coffee beans respectively. In the unroasted bean, HMF is localized to the silver skin within the loop and the thin layer on the outer surface of the bean. However, after roasting, HMF is more evenly distributed throughout the endosperm, with higher levels within the silver skin found in the inner loop. The spatial distribution patterns for furan and HMF were found to be consistent in different roasted coffee beans (Fig. S1).

The LADI-MS experiments were carried out using high-purity helium as the carrier gas instead of argon. Although in typical DART-HRMS analyses of whole coffee beans, furan and HMF are more readily detected using argon-DART, the two compounds are also observed using helium-DART. In the case of LADI-MS experiments, since the laser is ablating a relatively small area (70 μm^2) and produces a relatively small ablation plume, the protons generated in the open-air gap are not depleted by the presence of molecules with high proton affinities (such as caffeine) and therefore, furan and HMF are more readily detected by the LADI-MS experiments than by typical helium-DART-HRMS analysis of large pieces of coffee beans that are sampled directly.

The homogeneous distribution of furan within the entire tissue of the roasted coffee beans was not unexpected given that its proposed precursors would be expected to occur similarly. Furan can be formed by cyclization of aldotetrose derivatives derived from heat-promoted

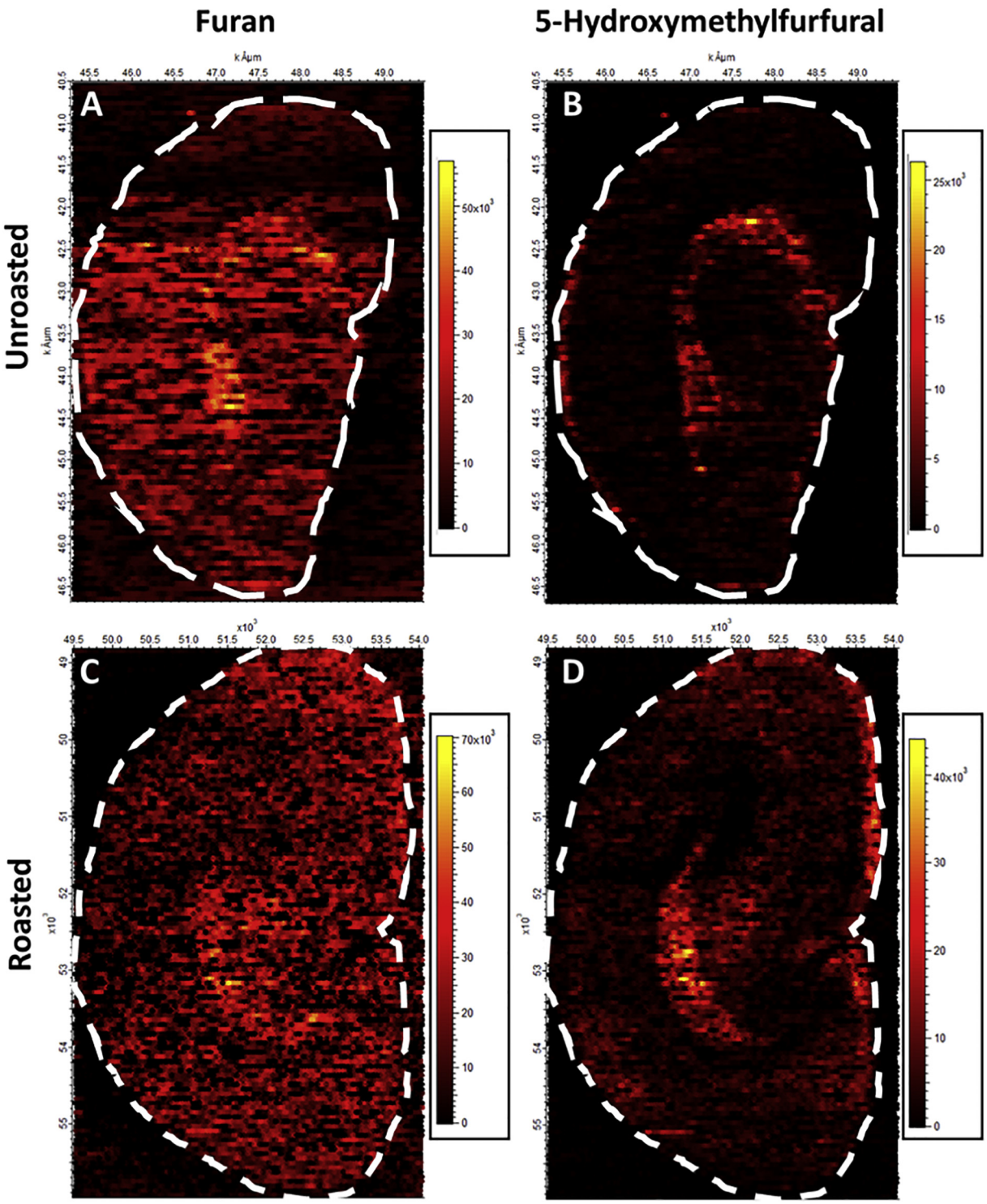

Fig. 6. The color-overlaid ion images of the *m/z* values corresponding to furan and 5-hydroxymethylfurfural in transverse cross-sections of unroasted (top) and roasted (bottom) coffee beans. Unroasted coffee bean: Panel A) furan; Panel B) 5-hydroxymethylfurfural. Roasted coffee bean: Panel C) furan; Panel D) 5-hydroxymethylfurfural. The color scale from black to yellow within each panel is indicative of zero or low intensity to a high intensity of the indicated ion. The white dashed line in each panel indicates the periphery of the coffee bean.

sugar degradation (Becalski & Seaman, 2005; Limacher et al., 2008; Maga & Katz, 1979; Perez Locas & Yaylayan, 2004), Maillard reactions between sugars and amino acids (Limacher et al., 2008; Owczarek-Fendor et al., 2010; Owczarek-Fendor et al., 2011; Perez Locas & Yaylayan, 2004; Van Lancker, Adams, Owczarek-Fendor, De Meulenaer, & De Kimpe, 2011), and thermal degradations of amino acids (Perez Locas & Yaylayan, 2004) among other pathways. All of these classes of precursor molecules would be expected to be represented throughout the coffee bean tissue. The homogeneous distribution of sucrose, for example, was demonstrated by Garrett et al. by desorption electrospray ionization-imaging mass spectrometry (DESI-IMS) (Garrett, Rezende, & Ifa, 2016). The anticipated broad occurrence of precursors provides a rationale for the homogenous distribution of furan in the roasted bean after heat treatment of the green beans. The

non-homogeneous occurrence of HMF is more intriguing. It too is proposed to be formed from carbohydrate and/or amino acid precursors that would be expected to be broadly distributed. Despite this, it is localized to the silver skin in the unroasted bean and to both the silver skin and the periphery in the roasted bean. This finding implies that either its precursors are localized to those areas, or that the regions where there is minimal to no HMF contain compounds that interfere with the formation of HMF and thus reduce its concentration. Studies of the molecular content of the silver skin may provide insight into some of the specific compounds that contribute to HMF formation in situ (as opposed to in model systems or experiments using model compounds), and this is the subject of ongoing studies in our laboratory. The finding that HMF is concentrated in the silver skin suggests that it may be possible to mitigate the formation of HMF by developing a green bean processing approach that involves removal of the areas such as the silver skin prior to roasting. This knowledge could not only eventually lead to the ability to track the production of desirable compounds as a function of species, cultivar and growth conditions, but also the ability to mitigate the production of undesirable molecules. The mechanism by which both furan and HMF are formed in the green beans is unclear, and the possibility that their formation is a function of the harvesting and processing of the green beans prior to roasting is also being investigated.

4. Conclusions

The spatial distribution maps of the small molecules furan and HMF in green and roasted coffee beans were determined. The presence of each analyte mapped by LADI-MS was supported by the independent confirmation of their presence by argon DART-HRMS and GC-TOF-MS. HMF was highly concentrated within the silver skin of the beans and distributed more widely after the roasting process. Furan, on the other hand, was widely distributed in both the green and roasted beans with higher levels in some areas of the silver skin. The findings indicate that while the precursors for furan formation appear in all parts of the bean, those for HMF may be localized to the silver skin. This information provides the opportunity to perform informed investigations of the chemical composition of those areas within the green bean which on heat treatment result in the formation of localized compounds such as HMF, and may lead to the development of methods for their potential removal during processing.

Acknowledgements

Thanks are extended to Elemental Scientific Lasers for the use of their Nd:YAG laser ablation system.

Funding

This work was supported in part by the United States National Institute of Justice [grant # 2017-R2-CX-0003]. The opinions, findings, and conclusions or recommendations expressed in this manuscript are those of the authors and do not necessarily reflect those of the Department of Justice.

Author contributions

RAM conceived of the project, supervised its implementation and wrote the manuscript with KLF. KLF completed LADI-MS experiments and performed GC–MS experiments. RBC and KO conducted argon-DART-HRMS and GC–MS experiments respectively.

Appendix A. Supplementary data

Supplementary data to this article can be found online at https://doi.org/10.1016/j.foodres.2018.10.052.

References

Anese, M. (2015). Furan and other furanic compounds in coffee: Occurrence, mitigation strategies, and importance of processing. In V. Preedy (Ed.). *Processing and Impact on active Components in Food* (pp. 541–547). San Diego: Academic Press.

Anese, M., Bot, F., & Suman, M. (2014). Furan and 5-hydroxymethylfurfural removal from high- and low-moisture foods. *LWT - Food Science and Technology, 56*(2), 529–532. https://doi.org/10.1016/j.lwt.2013.12.030.

Arisseto, A. P., Vicente, E., Ueno, M. S., Tfouni, S. A., & Toledo, M. C. (2011). Furan levels in coffee as influenced by species, roast degree, and brewing procedures. *Journal of Agricultural and Food Chemistry, 59*(7), 3118–3124. https://doi.org/10.1021/jf104868g.

Becalski, A., Halldorson, T., Hayward, S., & Roscoe, V. (2016). Furan, 2-methylfuran and 3-methylfuran in coffee on the Canadian market. *Journal of Food Composition and Analysis, 47*, 113–119. https://doi.org/10.1016/j.jfca.2016.01.006.

Becalski, A., & Seaman, S. (2005). Furan precursors in food: A model study and development of a simple headspace method for determination of furan. *Journal of AOAC International, 88*(1), 102–106.

Capuano, E., & Fogliano, V. (2011). Acrylamide and 5-hydroxymethylfurfural (HMF): A review on metabolism, toxicity, occurrence in food and mitigation strategies. *LWT - Food Science and Technology, 44*(4), 793–810. https://doi.org/10.1016/j.lwt.2010.11.002.

Conejero, G., Noirot, M., Talamond, P., & Verdeil, J. L. (2014). Spectral analysis combined with advanced linear unmixing allows for histolocalization of phenolics in leaves of coffee trees. *Frontiers in Plant Science, 5*, 39. https://doi.org/10.3389/fpls.2014.00039.

Crews, C., & Castle, L. (2007). A review of the occurrence, formation and analysis of furan in heat-processed foods. *Trends in Food Science and Technology, 18*(7), 365–372. https://doi.org/10.1016/j.tifs.2007.03.006.

De Castro, R. D., & Marraccini, P. (2006). Cytology, biochemistry and molecular changes during coffee fruit development. *Brazilian Journal of Plant Physiology, 18*, 175–199.

Dias, R. C., Campanha, F. G., Vieira, L. G., Ferreira, L. P., Pot, D., Marraccini, P., & De Toledo Benassi, M. (2010). Evaluation of kahweol and cafestol in coffee tissues and roasted coffee by a new high-performance liquid chromatography methodology. *Journal of Agricultural and Food Chemistry, 58*(1), 88–93. https://doi.org/10.1021/jf9027427.

Fowble, K. L., Teramoto, K., Cody, R. B., Edwards, D., Guarrera, D., & Musah, R. A. (2017). Development of “laser ablation direct analysis in real time imaging” mass spectrometry: Application to spatial distribution mapping of metabolites along the biosynthetic cascade leading to synthesis of atropine and scopolamine in plant tissue. *Analytical Chemistry, 89*(6), 3421–3429. https://doi.org/10.1021/acs.analchem.6b04137.

Garrett, R., Rezende, C. M., & Ifa, D. R. (2016). Revealing the spatial distribution of chlorogenic acids and sucrose across coffee bean endosperm by desorption electrospray ionization-mass spectrometry imaging. *LWT - Food Science and Technology, 65*(Supplement C), 711–717. https://doi.org/10.1016/j.lwt.2015.08.062.

Gökmen, V., Açar, Ö.Ç., Köksel, H., & Acar, J. (2007). Effects of dough formula and baking conditions on acrylamide and hydroxymethylfurfural formation in cookies. *Food Chemistry, 104*(3), 1136–1142. https://doi.org/10.1016/j.foodchem.2007.01.008.

Gökmen, V., & Şenyuva, H. Z. (2007). Effects of some cations on the formation of acrylamide and furfurals in glucose–asparagine model system. [journal article]. *European Food Research and Technology, 225*(5), 815–820. https://doi.org/10.1007/s00217-006-0486-7.

IARC (1995). *Furan Dry cleaning, some chlorinated solvents and other industrial chemicals. Vol. 63*, Lyon, France: World Health Organization393–407.

Kato, H., Hayase, F., Shin, D. B., Oimomi, M., & Baba, S. (1989). 3-Deoxyglucosone, an intermediate product of the Maillard reaction. *Progress in Clinical and Biological Research, 304*, 69–84.

Kroh, L. W. (1994). Caramelisation in food and beverages. *Food Chemistry, 51*(4), 373–379. https://doi.org/10.1016/0308-8146(94)90188-0.

Kuballa, T., Stier, S., & Strichow, N. (2005). Furan concentrations in coffee and coffee beverages. *Deutsche Lebensmittel-Rundschau, 101*, 229–235.

Lee, L. W., Cheong, M. W., Curran, P., Yu, B., & Liu, S. Q. (2016). Modulation of coffee aroma via the fermentation of green coffee beans with *Rhizopus oligosporus*: II. Effects of different roast levels. *Food Chemistry, 211*, 925–936. https://doi.org/10.1016/j.foodchem.2016.05.073.

Lee, L. W., Tay, G. Y., Cheong, M. W., Curran, P., Yu, B., & Liu, S. Q. (2017). Modulation of the volatile and non-volatile profiles of coffee fermented with *Yarrowia lipolytica*: I. Green coffee. *LWT - Food Science Technology, 77*, 225–232. https://doi.org/10.1016/j.lwt.2016.11.047.

Limacher, A., Kerler, J., Conde-Petit, B., & Blank, I. (2007). Formation of furan and methylfuran from ascorbic acid in model systems and food. *Food Additives and Contaminants, 24*(Suppl. 1), 122–135. https://doi.org/10.1080/02652030701393112.

Limacher, A., Kerler, J., Davidek, T., Schmalzried, F., & Blank, I. (2008). Formation of furan and methylfuran by Maillard-type reactions in model systems and food. *Journal of Agricultural and Food Chemistry, 56*(10), 3639–3647. https://doi.org/10.1021/jf800268t.

Maeztu, L., Sanz, C., Andueza, S., Paz De Peña, M., Bello, J., & Cid, C. (2001). Characterization of espresso coffee aroma by static headspace GC-MS and sensory flavor profile. *Journal of Agricultural and Food Chemistry, 49*(11), 5437–5444. https://doi.org/10.1021/jf0107959.

Maga, J. A., & Katz, I. (1979). Furans in foods. *Critical Reviews in Food Science and Nutrition, 11*(4), 355–400. https://doi.org/10.1080/10408397909527268.

Monien, B. H., Engst, W., Barknowitz, G., Seidel, A., & Glatt, H. (2012). Mutagenicity of 5-hydroxymethylfurfural in V79 cells expressing human SULT1A1: Identification and mass spectrometric quantification of DNA adducts formed. *Chemical Research in Toxicology, 25*(7), 1484–1492. https://doi.org/10.1021/tx300150n.

Moon, J.-K., & Shibamoto, T. (2009). Role of roasting conditions in the profile of volatile flavor chemicals formed from coffee beans. *Journal of Agricultural and Food Chemistry, 57*(13), 5823–5831. https://doi.org/10.1021/jf901136e.

Neuwirth, C., Mosesso, P., Pepe, G., Fiore, M., Malfatti, M., Turteltaub, K., ... Mally, A. (2012). Furan carcinogenicity: DNA binding and genotoxicity of furan in rats *in vivo*. *Molecular Nutrition & Food Research, 56*(9), 1363–1374. https://doi.org/10.1002/mnfr.201200226.

Owczarek-Fendor, A., De Meulenaer, B., Scholl, G., Adams, A., Van Lancker, F., Eppe, G., ... De Kimpe, N. (2011). Furan formation from lipids in starch-based model systems, as influenced by interactions with antioxidants and proteins. *Journal of Agricultural and Food Chemistry, 59*(6), 2368–2376. https://doi.org/10.1021/jf103168s.

Owczarek-Fendor, A., De Meulenaer, B., Scholl, G., Adams, A., Van Lancker, F., Yogendrarajah, P., ... De Kimpe, N. (2010). Importance of fat oxidation in starch-based emulsions in the generation of the process contaminant furan. *Journal of Agricultural and Food Chemistry, 58*(17), 9579–9586. https://doi.org/10.1021/jf101671u.

Perez Locas, C., & Yaylayan, V. A. (2004). Origin and mechanistic pathways of formation of the parent furan-a food toxicant. *Journal of Agricultural and Food Chemistry, 52*(22), 6830–6836. https://doi.org/10.1021/jf0490403.

Peterson, L. A. (2013). Reactive metabolites in the biotransformation of molecules containing a furan ring. *Chemical Research in Toxicology, 26*(1), 6–25. https://doi.org/10.1021/tx3003824.

Quarta, B., & Anese, M. (2012). Furfurals removal from roasted coffee powder by vacuum treatment. *Food Chemistry, 130*(3), 610–614. https://doi.org/10.1016/j.foodchem.2011.07.083.

Roman-Leshkov, Y., Chheda, J. N., & Dumesic, J. A. (2006). Phase modifiers promote efficient production of hydroxymethylfurfural from fructose. *Science, 312*(5782), 1933–1937. https://doi.org/10.1126/science.1126337.

Sijia, W., Enting, W., & Yuan, Y. (2014). Detection of furan levels in select Chinese foods by solid phase microextraction–gas chromatography/mass spectrometry method and dietary exposure estimation of furan in the Chinese population. *Food and Chemical Toxicology, 64*, 34–40. https://doi.org/10.1016/j.fct.2013.11.012.

Somorin, O. (1974). Caffeine distribution in *C. acuminata, T. cacao* and *C. arabica*. *Journal of Food Science, 39*(5), 1055–1056. https://doi.org/10.1111/j.1365-2621.1974.tb07310.x.

Van Lancker, F., Adams, A., Owczarek-Fendor, A., De Meulenaer, B., & De Kimpe, N. (2011). Mechanistic insights into furan formation in Maillard model systems. *Journal of Agricultural and Food Chemistry, 59*(1), 229–235. https://doi.org/10.1021/jf102929u.

Zanin, R. C., Corso, M. P., Kitzberger, C. S. G., Scholz, M. B.d. S., & Benassi, M.d. T. (2016). Good cup quality roasted coffees show wide variation in chlorogenic acids content. *LWT - Food Science and Technology, 74*, 480–483. https://doi.org/10.1016/j.lwt.2016.08.012.

Zheng, X.-q., & Ashihara, H. (2004). Distribution, biosynthesis and function of purine and pyridine alkaloids in *Coffea arabica* seedlings. *Plant Science, 166*(3), 807–813. https://doi.org/10.1016/j.plantsci.2003.11.024.